Published in final edited form as:
Nature. 2013 January 17; 493(7432): 424–428. doi:10.1038/nature11747.

Asymmetric neurotransmitter release enables rapid odor lateralization in *Drosophila*

Quentin Gaudry[1], **Elizabeth J. Hong**[1], **Jamey Kain**[2,3], **Benjamin L. de Bivort**[2,3], and **Rachel I. Wilson**[1]

[1] Department of Neurobiology, Harvard Medical School, 220 Longwood Ave., Boston, MA 02115

[2] Rowland Institute, Harvard University, 100 Edwin Land Boulevard, Cambridge, MA 02142

[3] Department of Organismic and Evolutionary Biology and Center for Brain Science, Harvard University, 52 Oxford St., Cambridge MA 02138

Abstract

In *Drosophila*, most individual olfactory receptor neurons (ORNs) project bilaterally to both sides of the brain[1,2]. Having bilateral rather than unilateral projections may represent a useful redundancy. However, bilateral ORN projections to the brain should also compromise the ability to lateralize odors. Nevertheless, walking or flying *Drosophila* reportedly turn toward their more strongly stimulated antenna[3-5]. Here we show that each ORN spike releases ~40% more neurotransmitter from the axon branch ipsilateral to the soma, as compared to the contralateral branch. As a result, when an odor activates the antennae asymmetrically, ipsilateral central neurons begin to spike a few milliseconds before contralateral neurons, and ipsilateral central neurons also fire at a 30-50% higher rate. We show that a walking fly can detect a 5% asymmetry in total ORN input to its left and right antennal lobes, and can turn toward the odor in less time than it requires the fly to complete a stride. These results demonstrate that neurotransmitter release properties can be tuned independently at output synapses formed by a single axon onto two target cells with identical functions and morphologies. Our data also show that small differences in spike timing and spike rate can produce reliable differences in olfactory behavior.

Insects navigating toward an odor can compare signals from their two antennae, and generally turn in the direction of the stronger signal. Confounding this strategy (by crossing and fixing the antennae, thereby spatially reversing them) impairs olfactory navigation in bees, ants, and locusts[6-8]. *Drosophila* resemble other insects in using this strategy[3-5], but they are unlike other insects in having mainly bilateral ORN projections. In the *Drosophila* brain, both ipsi- and contralateral ORN axons synapse onto antennal lobe projection neurons (PNs)[9], and ipsi- and contralateral synapses have approximately the same strength[10]. A minority of *Drosophila* olfactory glomeruli receive unilateral ORN projections[1,11], raising the question of whether these unilateral glomeruli are what enable lateralization.

To investigate lateralization behavior, we built a spherical treadmill to measure olfactory behavior in walking *Drosophila* (Fig. 1a and Supplementary Fig. 1). To prevent the head from moving, it was glued to the body, and the two antennae were independently stimulated with odor. When we delivered fermented peach volatiles to one antenna and clean air to the

Correspondence should be addressed to R.I.W. (rachel_wilson@hms.harvard.edu)..

Author Contributions: Q.G. and R.I.W. designed the experiments. Q.G. performed all the experiments, except for the calcium imaging, which was performed by Q.G. and E.J.H, and the synaptobrevin imaging, which was performed by R.I.W. Q.G. analyzed the data. J.K. and B.L.D. helped design and build the spherical treadmill apparatus. Q.G. and R.I.W. wrote the manuscript.

other, flies on the treadmill made a fictive turn toward the odor (Fig. 1b and c). If odor or clean air was delivered symmetrically to the two antennae, the fly continued to walk straight (Fig. 1d).

Fruit volatiles typically activate multiple ORN types[12]. Therefore, we next used a monomolecular odor (pentanoic acid) to more specifically target a glomerulus that receives bilateral ORN input. This odor has just one known high-affinity receptor in the antenna[11,12]. This receptor corresponds to glomerulus DM6, which receives bilateral ORN innervation[2,9]. Pentanoic acid elicited turning behavior as robust as that elicited by peach volatiles (Fig. 1d). Turning was significantly reduced by a mutation (*Orco*^{2}) which silences bilateral ORNs, including the DM6 ORNs (Fig. 1d). The ORN types that project unilaterally do not express the *Orco* gene[11,13], and so this result implies that asymmetric input to strictly bilateral glomeruli can produce turning.

To target a single bilateral ORN type more selectively, we expressed channelrhodopsin-2 (ChR2) in the ORNs that express the olfactory receptor Or42b and project to glomerulus DM1 (Fig. 1e). These ORNs fired a burst of 3 or 4 spikes during a 50-ms light pulse directed at the antenna with a fine fiber optic filament (Fig. 1f). In the same fly, light had no effect on adjacent ORNs that did not express ChR2 (Fig. 1f). Illuminating one antenna produced a turn toward the stimulus (Fig. 1g; Supplementary Figure 2). Conversely, light offset produced a compensatory turn in the other direction (Fig. 1g-i, Supplementary Information Footnote 1). The turns evoked by ChR2 in one ORN type were as large as when ChR2 was expressed in most ORN types (under the control of the *Orco-Gal4* line; Fig. 1h). Thus, bilateral ORNs can support lateralization behavior, and turning can be elicited by just a few spikes per neuron in one ORN type.

The temporal control enabled by the optogenetic approach allowed us to precisely determine the latency of the behavioral response. Surprisingly, turning began within ~ 70 ms of the ORN response onset (Fig. 1j). This is faster than the fly's stride period[14] (about 100 ms, Supplementary Fig. 1). Thus, there must be a rapid mechanism in the brain for extracting lateralized information from sensory neurons.

We next asked how asymmetric odor stimuli are encoded at the level of PN spikes. We removed one antenna in order to lateralize the odor stimulus, and we made simultaneous cell-attached recordings from PNs ipsi- and contralateral to the intact antenna (Fig. 2a, b). We recorded from pairs of PNs in the same glomerulus on different sides of the brain ("sister PNs"), using GFP to target our electrodes to PNs in glomerulus DM6 or DM1. We used odors that preferentially activate either DM6 ORNs or DM1 ORNs (pentanoic acid or dilute ethyl acetate[12]). In these experiments, we found a small but consistent asymmetry in PN odor responses. This was apparent in the latency to the first odor-evoked spike: the first ipsilateral spike occurred 2.47±0.70 ms earlier than the first contralateral spike in DM6 PNs, and 1.01±0.41 ms earlier in DM1 PNs (n=16 and 6, Fig. 2c). The latency difference was statistically significant for DM6 PN pairs, although it fell short of significance for DM1 PN pairs ($p < 0.005$ and $p = 0.06$, Wilcoxon signed-rank tests). In addition, we found an asymmetry in odour-evoked firing rates: ipsilateral firing rates were on average about 50% higher than contralateral firing rates for DM6 PNs, with a larger asymmetry for DM1 PNs (Fig. 2d–g). The asymmetry was observed even during the spontaneous firing of these cells, and it was proportionately similar for all odour concentrations (Fig. 2d, g). The asymmetry in spikes must be due to an asymmetry in synaptic currents. Indeed, asymmetric stimulation of the antennae produced systematically larger inward currents in ipsi- versus contralateral PNs (Supplementary Fig. 3).

Synaptic currents in PNs reflect the combined effects of ORNs and local neurons (LNs), most of which are GABAergic[15-17]. We first asked if the asymmetry in PN activity requires GABAergic inhibition, by bath-applying $GABA_A$ and $GABA_B$ receptor antagonists. These antagonists elevated PN firing rates, but the difference between ipsi- and contralateral PN firing rates was not significantly altered (Fig. 3a,b).

Our results suggest that the asymmetry originates at the level of ORN input to PNs. To compare ORN-to-PN synapses in ipsi- versus contralateral PNs, we made simultaneous whole-cell recordings of spontaneous excitatory postsynaptic currents (sEPSCs) in pairs of sister PNs. These sEPSCs are known to arise from ORN-to-PN synapses[9,10]. Each ORN-to-PN synapse consists of many release sites with high release probability, and so spike-evoked synaptic events are large and reliable[10]. In recordings from sister PNs in glomerulus DM6, virtually all sEPSCs occurred in a paired fashion (Fig. 3c). Almost 100% of the sEPSCs in one cell had a corresponding paired event in the other cell, and this percentage was not significantly different in ipsi- versus contralateral PNs (98.3 ± 0.6% versus 96.4 ± 1.3%, n = 15 pairs, $p = 0.11$, Wilcoxon signed-rank test). This result indicates that the number of unitary ORN-to-PN synaptic connections is essentially identical on the ipsi- and contralateral sides. This result also argues that action potential conduction failures do not occur to any appreciable degree in the contralateral axon branches of ORNs, although we cannot completely exclude the idea that this occurs at a low rate.

These dual whole-cell recordings allowed us to measure the mean difference in ipsi- versus contralateral sEPSC arrival times (0.80 ± 0.51 ms), which represents the delay imposed by axonal conduction between sister glomeruli. This delay is less than the contralateral lag in first spike latency in glomerulus DM6 (2.47 ms, see above). This makes sense, because the lag in first spike latency is the result of two delays: the delay imposed by axonal conduction, and the delay that results from less net synaptic excitation in the contralateral PN (Supplementary Fig. 3) which means that the contralateral PN requires more integration time to reach spike threshold.

Comparing the amplitude of paired sEPSCs on an event-by-event basis, we found considerable variation in the relative amplitude of ipsi- versus contralateral EPSCs (Fig. 3d). This is expected, given that synaptic vesicle release is a stochastic process occurring independently at ipsi- and contralateral synapses. When many sEPSCs were considered together, there was a consistent asymmetry in the amplitude of sEPSCs (Fig. 3d). Averaged across all experiments, ipsilateral sEPSCs were 39% larger than their contralateral counterparts (Fig. 3e). Thus, although ORN spikes reliably invade both ipsi- and contralateral axon branches, each ORN spike typically has a larger effect on ipsilateral PNs.

In principle, the asymmetry in sEPSC amplitudes could have either a pre- or postsynaptic locus. To determine if we can observe this asymmetry at the level of presynaptic release sites, we expressed synaptobrevin:GFP (a marker of presynaptic release sites) in DM6 ORNs. We removed one antenna and allowed three days for the cut ORN axons to degenerate, leaving only the axons from the intact antenna. We found that total synaptobrevin fluorescence was on average 41 ± 16% higher on the ipsilateral side, and the ipsi/contra ratio of synaptobrevin fluorescence was significantly greater than 1 ($p < 0.05$, n = 5, t-test, Fig. 4a). This suggests an asymmetry in the number or size of neurotransmitter release sites. This is consistent with a previous study reporting that a plasma membrane marker was more abundant on the ipsilateral side[18]. That study also severed one antenna and waited three days before imaging. Functional remodeling can occur over that time period[18,19], so both findings should be interpreted cautiously.

Next, to visualize presynaptic calcium, we expressed the genetically-encoded calcium indicator GCaMP3.0 in ORNs (using the *pebbled-Gal4* line) and used two-photon microscopy to visualize calcium signals in ORN axon terminals. To lateralize the odor, we removed one antenna immediately prior to the experiment (Fig. 4b). We used pentanoic acid to evoke a fluorescence increase preferentially in glomerulus DM6 (Fig. 4c). We found that the size of the calcium response was significantly larger on the side of the brain ipsilateral to the intact antenna (Fig. 4c and d). This asymmetry did not require feedback from central circuits, because it persisted after washing in mecamylamine (to block nicotinic acetylcholine receptors, which mediate ORN-to-PN synaptic transmission[10]) along with picrotoxin and CGP54626 (Fig. 4e). In separate experiments, we saw similarly asymmetric calcium signals in glomerulus DL5, using an odor stimulus which is relatively selective for DL5 ORNs[20] (trans-2-hexenal, 10^{-5} dilution, data not shown). We also saw a similar asymmetry in presynaptic currents, using simultaneous bilateral field potential recordings (Supplementary Figure 4). Together, these results demonstrate that the asymmetry in EPSC amplitudes has a presynaptic origin.

Interestingly, we found a roughly equal asymmetry (~40%) in the amplitude of sEPSCs, the level of synaptobrevin fluorescence, and the odour-evoked GCaMP3 fluorescence change. The simplest explanation for these results is that the ipsilateral arbor is 40% larger than the contralateral arbor. If everything else is equal, then this mechanism should produce a proportional change in all these measurements (Supplementary Information Note 2).

Our results are consistent with the finding that, in flies with one antenna removed, 2-deoxyglucose uptake is higher on the side ipsilateral to the intact antenna[21]. A previous study using calcium imaging has reported that asymmetric ORN stimulation can produce stronger signals in ipsilateral PNs than in contralateral PNs[22], which is also broadly consistent with our results. In contrast to our results, however, this asymmetry was restricted to just a few glomeruli. This finding is puzzling, given that a variety of stimuli can produce turning behavior (Fig. 1 and refs [3-5]). The same study also concluded that GABAergic inhibition mediates the ipsi/contra asymmetry in PNs[22]. These discrepancies may reflect limitations of the imaging techniques used in that study, as well as differences between stimuli or glomeruli.

Another previous study failed to find any significant ipsi-contra differences in the strength of ORN-PN synapses[10]. Those measurements involved sequential recordings from sister PNs, rather than simultaneous recordings. Also, that study measured EPSCs arising from a single ORN per PN. Here, we have better statistical power because we made simultaneous recordings from sister PNs, and because we sampled sEPSCs arising from many ORNs. Our finding that ipsi- and contralateral synapses differ only modestly explains why this difference has been difficult to resolve previously.

It is well-known that a single axon can form neurotransmitter release sites with different properties onto different target cell types (e.g., principal neurons versus interneurons)[23]. Here, we have shown that ORN axons discriminate between two classes of target cells (left and right) that are morphologically and functionally identical, and that share the same lineage and birth dates[24]. This is reminiscent of the circuitry of the leech midbody ganglion, where individual mechanoreceptor axons make stronger synapses onto ipsi- versus contralateral sister cells that are otherwise functionally identical[25]. How are these target cells distinguished? Right and left sister neurons might express different molecular tags[26], thereby allowing a given axon to recognize them as ipsi- versus contralateral to itself. Alternatively, an axon might form more release sites at proximal locations as compared to distal locations; this cell-intrinsic mechanism would suffice because contralateral sites are always more distal than ipsilateral sites.

Our results reveal that even small signals in the *Drosophila* nervous system can be behaviorally relevant. The stimuli we used in our optogenetic experiments produced only a slight fractional difference in input to the right and left sides of the brain. This difference amounted to 5% over the 50-ms stimulus period (Supplementary Information Footnote 3). The finding that this incremental difference is relevant for behavior should motivate the continued development of sensitive methods for monitoring neural activity in the fly brain.

Methods Summary

The odor delivery device used for the olfactory behavioral experiments was specially designed to deliver no lateralized mechanical cues, and we performed control experiments to confirm that no turning was observed when no odor was present (Supplementary Fig. 5). The spherical treadmill apparatus was constructed by floating a small plastic sphere on a jet of compressed air. We measured the forward and lateral velocities of the sphere in the apparatus by placing the sensor from an optical mouse underneath the sphere. Photostimulation of *Drosophila* ORNs was achieved by butt-coupling a blue LED to a fiber optic filament (50 μm diameter) and positioning the tip of the fiber ~150 μm away from the fly's antenna. In all behavioral experiments using light to stimulate ORNs, the eyes and ocelli of the fly were shielded from light by painting them with ink. *In vivo* extracellular recordings from ORNs and patch-clamp recordings from PNs were performed as previously described[9,27]. In all electrophysiology or calcium imaging experiments (except ORN recordings), one antenna was removed just prior to the experiment by a person who was not the experimenter, and the experimenter remained blind to which side of the brain was ipsilateral to the intact antenna. All analysis was also performed blind to which side was ipsilateral. Calcium imaging experiments were performed on a custom-built two-photon microscope. All measurements represent mean ± s.e.m. computed across experiments. See Supplementary Methods for details on the spherical treadmill, odor delivery, optogenetic stimuli, and analysis of sEPSCs.

Supplementary Material

Refer to Web version on PubMed Central for supplementary material.

Acknowledgments

We are grateful to Michael Dickinson, Vivek Jayaraman, Liqun Luo, Dan Tracey, and Leslie Vosshall for gifts of fly stocks. Allison Baker helped construct and improve the spherical treadmill apparatus. Members of the Wilson lab provided feedback on the manuscript. This work was supported by a research project grant from the National Institutes of Health (R01DC008174). R.I.W. is an HHMI Early Career Scientist. B.D. and J.K. were supported by the Rowland Junior Fellows Program.

References

1. Stocker RF, Lienhard MC, Borst A, Fischbach KF. Neuronal architecture of the antennal lobe in Drosophila melanogaster. Cell Tissue Res. 1990; 262:9–34. [PubMed: 2124174]
2. Couto A, Alenius M, Dickson BJ. Molecular, anatomical, and functional organization of the Drosophila olfactory system. Curr. Biol. 2005; 15:1535–1547. [PubMed: 16139208]
3. Borst A, Heisenberg M. Osmotropotaxis in Drosophila melanogaster. J. Comp. Physiol. [A]. 1982; 147:479–484.
4. Duistermars BJ, Chow DM, Frye MA. Flies require bilateral sensory input to track odor gradients in flight. Curr. Biol. 2009; 19:1301–1307. [PubMed: 19576769]
5. Flugge C. Geruchliche Raumorientierung von Drosophila melanogaster. Z. Vergl. Phys. 1934; 20:463–500.

6. Kennedy JS, Moorehouse JE. Laboratory observations on locust responses to wind-borne grass odour Entomol. Exp. Appl. 1969; 12:487–503.
7. Martin H. Osmotropotaxis in the honey-bee. Nature. 1965; 208:59–63.
8. Hangartner W. Spezifität und Inaktivierung des Spurpheromons von Lasius fuliginosus (Latr.) und Orientierung der Arbeiterinnen im Duftfeld. Z. vergl. Physiol. 1967; 57:103–136.
9. Kazama H, Wilson RI. Origins of correlated activity in an olfactory circuit. Nat. Neurosci. 2009; 12:1136–1144. [PubMed: 19684589]
10. Kazama H, Wilson RI. Homeostatic matching and nonlinear amplification at genetically-identified central synapses. Neuron. 2008; 58:401–413. [PubMed: 18466750]
11. Silbering AF, et al. Complementary function and integrated wiring of the evolutionarily distinct Drosophila olfactory subsystems. J Neurosci. 2011; 31:13357–13375. [PubMed: 21940430]
12. Hallem EA, Carlson JR. Coding of odors by a receptor repertoire. Cell. 2006; 125:143–160. [PubMed: 16615896]
13. Benton R, Vannice KS, Gomez-Diaz C, Vosshall LB. Variant ionotropic glutamate receptors as chemosensory receptors in Drosophila. Cell. 2009; 136:149–162. [PubMed: 19135896]
14. Strauss R, Heisenberg M. Coordination of legs during straight walking and turning in Drosophila melanogaster. J Comp Physiol A. 1990; 167:403–412. [PubMed: 2121965]
15. Chou YH, et al. Diversity and wiring variability of olfactory local interneurons in the Drosophila antennal lobe. Nat. Neurosci. 2010; 13:439–449. [PubMed: 20139975]
16. Okada R, Awasaki T, Ito K. Gamma-aminobuyric acid (GABA)-mediated neural connections in the Drosophila antennal lobe. J. Comp. Neurol. 2009; 514:74–91. [PubMed: 19260068]
17. Das A, et al. Drosophila olfactory local interneurons and projection neurons derive from a common neuroblast lineage specified by the empty spiracles gene. Neural Dev. 2008; 3:33. [PubMed: 19055770]
18. Berdnik D, Chihara T, Couto A, Luo L. Wiring stability of the adult Drosophila olfactory circuit after lesion. J. Neurosci. 2006; 26:3367–3376. [PubMed: 16571743]
19. Kazama H, Yaksi E, Wilson RI. Cell death triggers olfactory circuit plasticity via glial signaling in Drosophila. J. Neurosci. 2011; 31:7619–7630. [PubMed: 21613475]
20. Olsen SR, Bhandawat V, Wilson RI. Divisive normalization in olfactory population codes. Neuron. 2010; 66:287–299. [PubMed: 20435004]
21. Rodrigues V. Spatial coding of olfactory information in the antennal lobe of Drosophila melanogaster. Brain Res. 1988; 453:299–307. [PubMed: 3135918]
22. Agarwal G, Isacoff E. Specializations of a pheromonal glomerulus in the Drosophila olfactory system. J. Neurophysiol. 2011; 105:1711–1721. [PubMed: 21289134]
23. Pelkey KA, McBain CJ. Differential regulation at functionally divergent release sites along a common axon. Curr. Opin. Neurobiol. 2007; 17:366–373. [PubMed: 17493799]
24. Jefferis GS, Marin EC, Stocker RF, Luo L. Target neuron prespecification in the olfactory map of Drosophila. Nature. 2001; 414:204–208. [PubMed: 11719930]
25. Lockery SR, Kristan WB Jr. Distributed processing of sensory information in the leech. II. Identification of interneurons contributing to the local bending reflex. J. Neurosci. 1190; 10:1816–1829. [PubMed: 2355252]
26. Chintapalli VR, et al. Functional correlates of positional and gender-specific renal asymmetry in Drosophila. PLoS One. 2012; 7:e32577. [PubMed: 22496733]
27. Bhandawat V, Olsen SR, Schlief ML, Gouwens NW, Wilson RI. Sensory processing in the Drosophila antennal lobe increases the reliability and separability of ensemble odor representations. Nat. Neurosci. 2007; 10:1474–1482. [PubMed: 17922008]
28. Bhandawat V, Maimon G, Dickinson MH, Wilson RI. Olfactory modulation of flight in Drosophila is sensitive, selective and rapid. J. Exp. Biol. 2010; 213:3625–3635. [PubMed: 20952610]
29. Fishilevich E, Vosshall LB. Genetic and functional subdivision of the Drosophila antennal lobe. Curr. Biol. 2005; 15:1548–1553. [PubMed: 16139209]
30. Larsson MC, et al. Or83b encodes a broadly expressed odorant receptor essential for Drosophila olfaction. Neuron. 2004; 43:703–714. [PubMed: 15339651]

31. Hwang RY, et al. Nociceptive neurons protect Drosophila larvae from parasitoid wasps. Curr. Biol. 2007; 17:2105–2116. [PubMed: 18060782]

32. Tanaka NK, Awasaki T, Shimada T, Ito K. Integration of chemosensory pathways in the Drosophila second-order olfactory centers. Curr. Biol. 2004; 14:449–457. [PubMed: 15043809]

33. Lee T, Luo L. Mosaic analysis with a repressible cell marker for studies of gene function in neuronal morphogenesis. Neuron. 1999; 22:451–461. [PubMed: 10197526]

34. Zhang YQ, Rodesch CK, Broadie K. Living synaptic vesicle marker: synaptotagmin-GFP. Genesis. 2002; 34:142–145. [PubMed: 12324970]

35. Sweeney LB, et al. Temporal target restriction of olfactory receptor neurons by Semaphorin-1a/PlexinA-mediated axon-axon interactions. Neuron. 2007; 53:185–200. [PubMed: 17224402]

36. Tian L, et al. Imaging neural activity in worms, flies and mice with improved GCaMP calcium indicators. Nat. Methods. 2009; 6:875–881. [PubMed: 19898485]

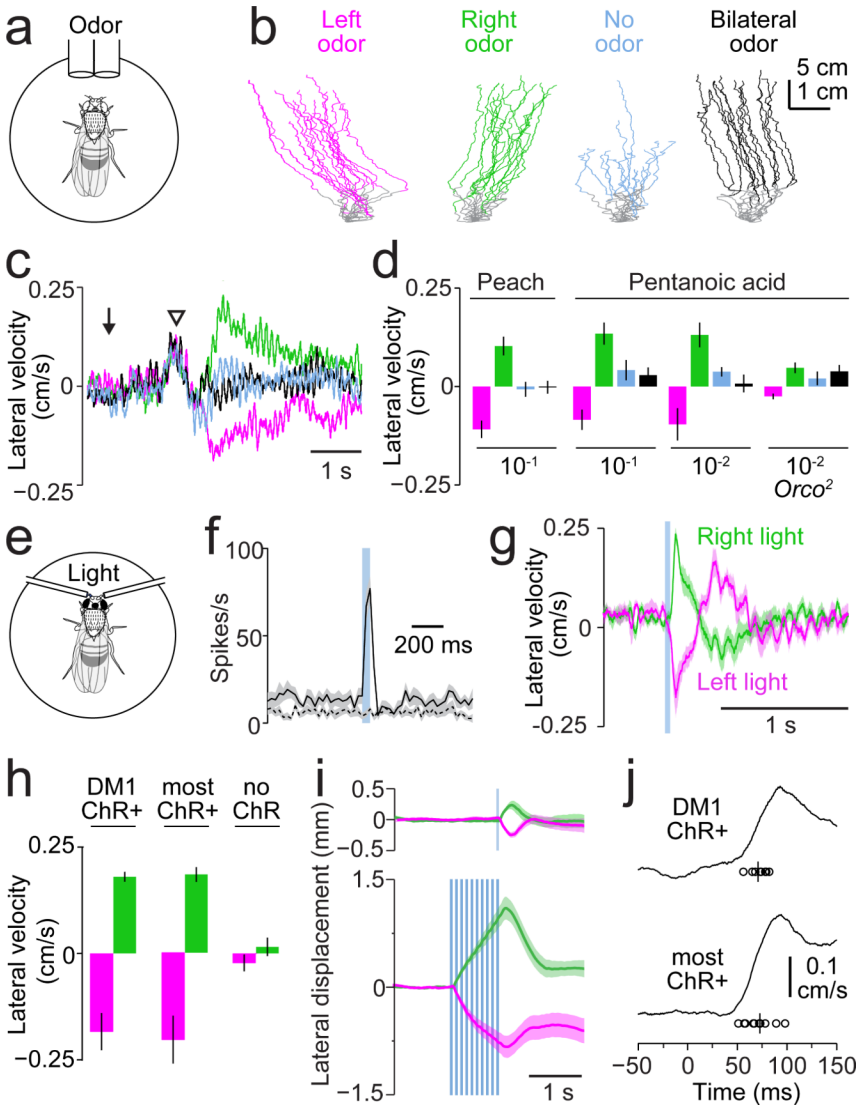

Figure 1.

Drosophila can lateralize odors based on bilateral receptor neuron input to a single pair of glomeruli. **a**. Schematic diagram of a fly on a spherical treadmill, with odor tubes directed at each antenna. **b**. Representative running trajectories from a single fly. Each trace is a different trial lasting 20 s. The gray portion of each trace indicates the pre-odor baseline period. Flies turn toward lateralized odor (fermented peach extract), but otherwise tend to run straight. **c**. Time course of mean lateral velocity in olfactory stimulation experiments (n = 9 flies). Positive values denote rightward turns and negative values denote leftward turns. Arrow indicates the onset of air flow through the tubing. The open arrowhead shows where clean air from the tip of the olfactometer first reaches the flies; this elicits a rightward turn which reflects either a systematic asymmetry in the tethering of the flies or an inherent handedness in the flies. Once this clean air is evacuated, odorized air elicits asymmetrical turning in the fly. Oscillations in lateral velocity are caused by the fly's stride rhythm (Supplementary Figure 1). Color key same as panel b. **d**. Mean lateral velocity (± s.e.m.) is significantly different for right versus left odor (green versus magenta bars). This was true for peach odor (10^{-1} dilution, $p < 0.005$, $n = 9$ flies, Wilcoxon signed-rank test). It was also true for pentanoic acid (10^{-1} and 10^{-2} dilutions, $n = 8$ and 12, $p < 0.01$ and $p < 0.005$,

Wilcoxon signed-rank tests). In *Orco*^{2} mutant flies, responses to right and left odor were still significantly different (n = 12 flies, $p < 0.005$, Wilcoxon signed-rank test) but were much smaller. The average difference between left and right (computed within each fly) is significantly smaller in *Orco*^{2} flies compared to control flies ($p < 0.05$, Mann-Whitney U test). The residual response in the mutants is likely due to the ORNs which do not rely on *Orco* (refs[11,13]). **e**. Schematic diagram of a fly on a spherical treadmill, with a fiber-optic light guide directed at each antenna. **f**. Time course of mean light-evoked firing rate in DM1 ORNs (ChR+, solid line) versus other ORN types (ChR-, dashed line). Shaded bands here and elsewhere represent ± s.e.m. **g**. Time course of mean lateral velocity during optogenetic stimulation in flies where DM1 ORNs are ChR2+. **h**. Mean lateral velocity is significantly different for left and right antennal illumination in flies where DM1 ORNs are ChR2+, or in flies where most ORNs are ChR2+ (n = 10 and 12, $p < 0.005$ and $p < 5\times10^{-4}$, Wilcoxon signed-rank tests), but not in flies where no ORNs express ChR2 ($p = 0.13$, $n = 10$). To express ChR2 in most ORNs, we used the *Orco-Gal4* line. Flies that lack ChR2 expression have the *UAS-ChR2* transgene but no Gal4 transgene. **i**. Time course of mean lateral displacement in response to a single light pulse (top) or a train of pulses (bottom). After the train, the magnitude of the compensatory turn is larger ($p < 0.005$, t-test), but the flies are also significantly less accurate in returning to their original running trajectory ($p < 0.005$, t-test). **j**. Time course of absolute mean lateral velocity on an expanded scale around the time of light onset (0 ms). Open circles show the turning latency for each fly. The mean latency across flies is shown as a vertical bar.

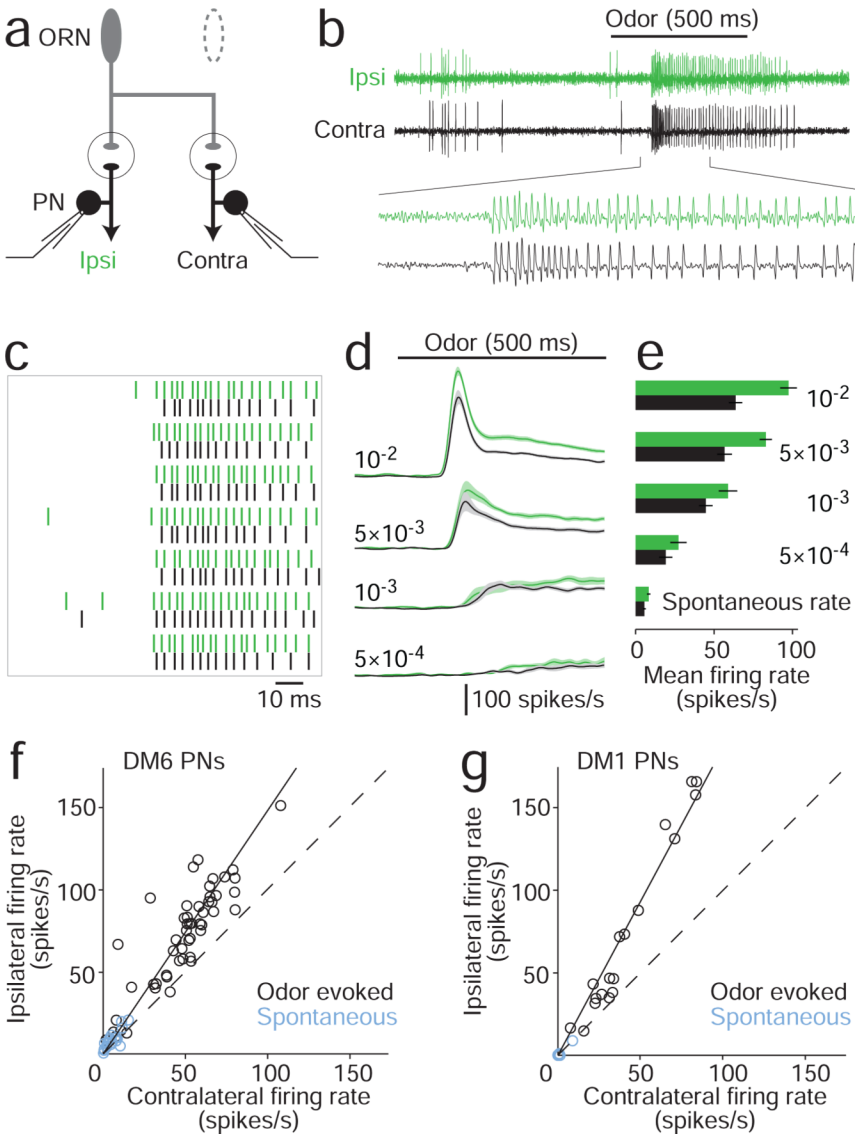

Figure 2.

Lateralized odors produce an asymmetry in spike latency and spike rate in antennal lobe projection neurons. **a**. Schematic of simultaneous cell-attached recording configuration. An ORN axon innervates a glomerulus on each side of the midline, where it synapses onto postsynaptic PNs. In these experiments, one antenna was removed to lateralize the odor. **b**. Sample cell-attached recordings from a pair of PNs (postsynaptic to glomerulus DM6). The odor stimulus is a 500-ms pulse of pentanoic acid (10^{-2} dilution). Enlarged segment below is 250 ms. **c**. Raster plot showing the spiking responses of ipsi- and contralateral DM6 PNs (odor is pentanoic acid 10^{-2}). Each pair of rows represents a single trial from the same pair of neurons. The raster starts 180 ms after the nominal odor pulse onset. Note the shorter ipsilateral latency (see text). **d**. Time course of mean firing rates of DM6 PNs to a descending series of pentanoic acid concentrations. **e**. Mean firing rates of DM6 PNs (± s.e.m.) in response to pentanoic acid concentrations. Spontaneous rates are also shown. Mean rate is computed over a 500 ms period starting 100 ms after the olfactometer is activated (n = 16, 15, 10, 10, and 21 pairs, in descending order of concentration). **f**. Trial-averaged ipsilateral versus contralateral firing rates for DM6 PNs. Several odor

concentrations were used in each experiment, and each point represents a different experiment-concentration combination. Note that the ipsi/contra difference is present in spontaneous activity (blue symbols). Significance was assessed by fitting a line through the origin to the data for each individual experiment; these slopes were significantly different from unity (mean slope = 1.47 ± 0.09, $p < 10^{-4}$, Mann-Whitney U test, $n = 21$ experiments). The dashed line is unity; the solid line is the mean of all linear fits in the individual experiments. **g**. Same as f, for DM1 PNs (mean slope = 1.86 ± 0.04, $p < 0.05$, Mann-Whitney U test, $n = 6$ experiments). Odor stimuli were ethyl acetate at 10^{-12}, 10^{-10}, and 10^{-6} dilutions. In DM1 PNs, spontaneous firing rates are close to zero.

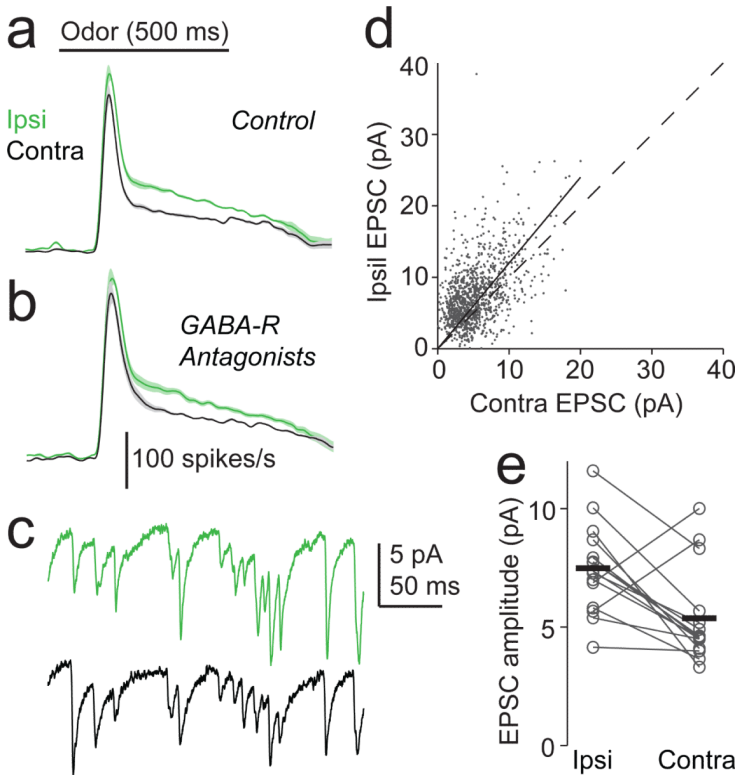

Figure 3.

The asymmetry arises at the level of ORN-to-PN synapses. **a**. Mean DM6 PN responses to pentanoic acid (10^{-2}) in normal saline. **b**. Same as (a) after adding the $GABA_A$ receptor antagonist picrotoxin (5 μM) and the $GABA_B$ receptor antagonist CGP54626 (50 μM). Ipsilateral firing rates are significantly higher than contralateral rates, ($p < 0.01$) and the antagonists have no significant effect on the ipsi/contra difference ($p = 0.86$, $n = 10$, 2-way ANOVA on data from panels a and b). The ipsi/contra difference in peak firing rates becomes somewhat smaller, but because this occurs only at the peak, it is likely due to the near-saturation of PN firing rates. **c**. Whole-cell recordings of spontaneous EPSCs from a pair of DM6 PNs. The PN ipsilateral to the intact antenna is in green. **d**. Ipsi- versus contralateral EPSC amplitudes in a typical pair of DM6 PNs. Each point represents a pair of EPSCs ($n = 1{,}213$). Dashed line is unity; solid line is a linear fit constrained to intersect the origin. **e**. Group data showing mean spontaneous EPSC amplitudes in all pairs of DM6 PNs. Each symbol is a different experiment and horizontal lines represent means across experiments. EPSC amplitudes are significantly larger in ipsilateral PNs ($n = 15$ pairs, $p < 0.05$,Wilcoxon signed-rank test).

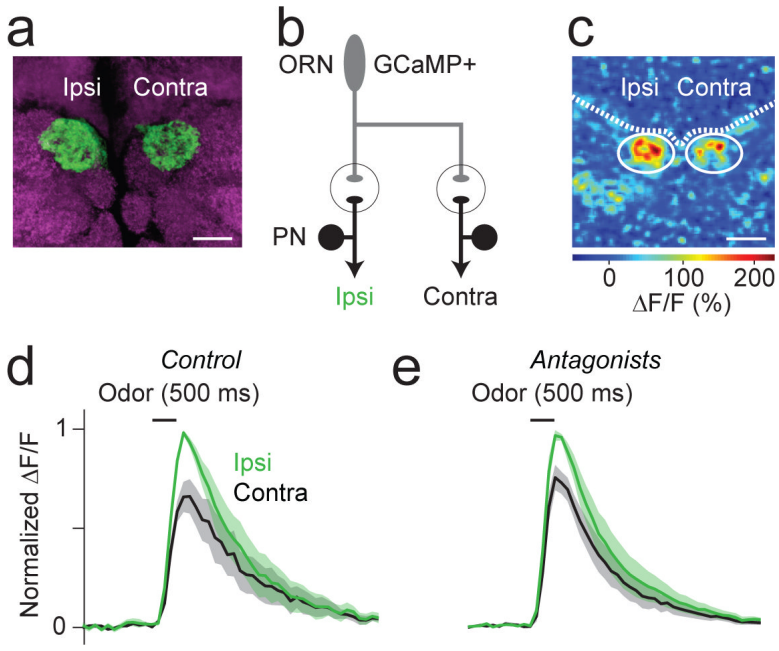

Figure 4.

The asymmetry in ORN-to-PN synapses has a presynaptic origin. **a**. Synaptobrevin:GFP (green) was expressed in DM6 ORNs to label neurotransmitter release sites, and one antenna was removed 3 days prior to allow the cut axons to degenerate. The brain is viewed from the anterior face. Magenta shows neuropil contours (nc82 immunofluorescence). Scale bar is 10 μm. **b**. Schematic of calcium recording configuration. ORNs express GCaMP, and one antenna was removed to lateralize the odor. **c**. Changes in fluorescence in ORN axon terminals in response to 10^{-2} pentanoic acid. Solid circles outline the DM6 glomeruli, and the dashed line shows the anterior boundary of the antennal lobe neuropil. The brain is viewed from the dorsal side. Scale bar is 10 μm. **d**. Mean time course of odor-evoked calcium signals in ORN axons innervating glomerulus DM6. Black bar indicates the timing of the odor stimulus (pentanoic acid 10^{-2}, 500 ms). **e**. Same as (d) except after adding picrotoxin, CGP54626, and the nicotinic receptor antagonist mecamylamine (200 μM). Ipsilateral responses are significantly larger than contralateral responses ($p < 0.05$) and the antagonists have no significant effect on the ipsi/contra difference ($p = 0.75$, $n = 6$, 2-way ANOVA on data from panels d and e).